

Hierarchic-EEG2Text: Assessing EEG-To-Text Decoding across Hierarchical Abstraction Levels

Anupam Sharma
sharmaanupam@iitgn.ac.in
IIT Gandhinagar
Gandhinagar, Gujarat, India

Harish Katti
kattih2@nih.gov
NIMH, NIH
USA

Prajwal Singh
singh_prajwal@iitgn.ac.in
IIT Gandhinagar
Gandhinagar, Gujarat, India

Shanmuganathan Raman
shanmuga@iitgn.ac.in
IIT Gandhinagar
Gandhinagar, Gujarat, India

Krishna Miyapuram
kprasad@iitgn.ac.in
IIT Gandhinagar
Gandhinagar, Gujarat, India

Abstract

An electroencephalogram (EEG) records the spatially averaged electrical activity of neurons in the brain, measured from the human scalp. Prior studies have explored EEG-based classification of objects or concepts, often for passive viewing of briefly presented image or video stimuli, with limited classes. Because EEG exhibits a low signal-to-noise ratio, recognizing fine-grained representations across a large number of classes remains challenging; however, abstract-level object representations may exist. In this work, we investigate whether EEG captures object representations across multiple hierarchical levels, and propose episodic analysis, in which a Machine Learning (ML) model is evaluated across various, yet related, classification tasks (episodes). Unlike prior episodic EEG studies that rely on fixed or randomly sampled classes of equal cardinality, we adopt hierarchy-aware episode sampling using *WordNet* to generate episodes with variable classes of diverse hierarchy. We also present the largest episodic framework in the EEG domain for detecting observed text from EEG signals in the PEERS dataset, comprising 931538 EEG samples under 1610 object labels, acquired from 264 human participants (subjects) performing controlled cognitive tasks, enabling the study of neural dynamics underlying perception, decision-making, and performance monitoring.

We examine how the semantic abstraction level affects classification performance across multiple learning techniques and architectures, providing a comprehensive analysis. The models tend to improve performance when the classification categories are drawn from higher levels of the hierarchy, suggesting sensitivity to abstraction. Our work highlights abstraction depth as an underexplored dimension of EEG decoding and motivates future research in this direction.

CCS Concepts

• Applied computing → Bioinformatics; • Computing methodologies → Multi-task learning.

Keywords

EEG2Text, BCI, Hierarchical Modeling, Meta-Learning

1 Introduction

Electroencephalography (EEG) is a non-invasive and cost-effective technique for measuring electrical activity in the human brain. EEG records spatially averaged electrical activity across the dendrites of

neurons in the underlying brain tissue, measured from the human scalp via electrodes [6]. Due to spatial averaging, EEG does not capture all underlying neural activity, limiting the amount of fine-grained information that can be recovered from the signal [6].

Despite these limitations, several studies have attempted to develop machine learning (ML) models that map EEG signals to the corresponding stimuli. Often, the stimuli are visual, and EEG is recorded while humans passively view images from a fixed set of categories. In these settings, ML models are trained to classify EEG signals into the corresponding category [15, 23, 24, 27, 30, 38], where the number of categories typically ranges from 10 to 80. In other studies, EEG signals are mapped to visually presented words or text [12, 13, 18, 28], where the number of categories equals the vocabulary size, which can be in the thousands. For example, the Zuco dataset [12] contains approximately 21K words.

While these studies demonstrate that EEG contains information related to the presented stimulus, our findings show that decoding performance degrades as the number of categories increases. This raises a fundamental question: rather than asking if EEG can support fine-grained classification over a large label space, we ask how much information it captures at varying levels of abstraction. Prior work in cognitive neuroscience has shown that neural representations of objects during visual processing evolve hierarchically over time [3, 5]. However, most EEG decoding studies evaluate performance using a flat label space, without explicitly considering the semantic hierarchy among categories. We further note that many existing datasets rely on abrupt presentation of visual stimuli, such as images or videos, during passive viewing tasks. Such stimuli are likely to elicit stereotyped brain responses across large regions [35], which may benefit classification models but may not reflect real-world perception, decision-making, or performance monitoring. In contrast, tasks involving real-world object concepts are likely to introduce greater subjectivity across participants. In this work, we investigate whether EEG captures abstract, hierarchical representations of objects during such challenging real-world tasks. Instead of evaluating models jointly across all categories, we propose an episodic evaluation framework in which each episode consists of a smaller classification task. Unlike most episodic learning studies in the EEG domain, which construct episodes from random samples, we design episodes that follow a semantic hierarchy. This allows us to probe EEG representations at multiple levels of abstraction.

To this end, we leverage the Penn Electrophysiology of Encoding and Retrieval Study (PEERS) dataset [14], which consists of EEG signals recorded while participants viewed approximately 1.6K words representing real-world objects. The large vocabulary and number of samples make this dataset suitable for episodic analysis. To construct the semantic hierarchy, we use NLTK’s WordNet [2, 32], which links words and concepts via the *IS-A* relationship. WordNet groups synonyms into synsets, and synsets are connected via *IS-A* relations, which we use to build a Directed Acyclic Graph (DAG). The leaf nodes correspond to words in the PEERS dataset, while internal nodes represent synsets. Each internal node defines a classification task over its descendant leaf nodes, and sampling nodes at different depths of the DAG yields episodes at varying levels.

By using this strategy, we construct the largest episodic EEG-to-text decoding framework, comprising 931538 EEG samples under 1610 labels from 264 subjects. We evaluate both non-episodic and episodic approaches, including meta-learning algorithms, across multiple modern architectures. Our results show that while modern architectures (even with self-supervised pretraining) fail under non-episodic evaluation, they perform comparatively better, though near chance, under hierarchical episodic evaluation. Moreover, performance improves as fine-grained classes are replaced with more abstract classes. These findings suggest that while EEG may not capture fine-grained representations, it does encode information at higher levels of semantic abstraction. Our contribution is a controlled evaluation framework that systematically examines which levels of semantic abstraction are accessible from the EEG during realistic cognitive tasks.

2 Background

This section briefly introduces the evaluation and learning approaches used in our work.

2.1 Episodic Vs Non-Episodic Evaluation

2.1.1 Non-Episodic Evaluation. In this work, we refer to the evaluation of an ML model in a typical classification task as non-episodic evaluation. Assume a Deep Neural Network (DNN) model trained for classifying samples into a set of classes C_{train} . When the model is evaluated on the task, the set of classes in the test set C_{eval} typically remains the same as C_{train} , and the number of units in the network’s last layer doesn’t change during testing.

2.1.2 Episodic Evaluation. Assume a DNN model trained for classifying samples into a set of classes C_{train} is tested on a new classification task with a set of classes C_{eval} where $|C_{eval} - C_{train}| \geq 1$. In such cases, the last layer needs to be replaced with number of units equal to C_{eval} and the model parameters needs to be updated using set of some samples $\mathcal{S} = \{(x_1, y_1), (x_2, y_2), \dots (x_K, y_K)\}$ from the new task and then the performance is evaluated on the set of unseen samples of that task $\mathcal{Q} = \{(x_1^*, y_1^*), (x_2^*, y_2^*), \dots (x_T^*, y_T^*)\}$. Here \mathcal{S} and \mathcal{Q} are known as the *Support Set* and *Query Set* respectively. When, $|C_{eval}| = N$ and the number of samples per class, $k_c = k$, we refer the task as "*N*-way, *k*-shot" classification task. When a model is evaluated on numerous such tasks independently, we call it episodic evaluation, where each task is referred to as an episode.

2.2 Episodic Learning Approaches

There exist many episodic learning approaches, out of which we focus mainly on meta-learning algorithms. Meta-learning is the ability of a model (or learner) to gain experience across multiple tasks (or episodes), such that, given a new episode with a very few samples, it quickly adapts. Here, we select episodic gradient-based meta-learning approaches, specifically Model-Agnostic Meta-Learning (MAML) [10] and its variants. In the context of gradient-based methods, the term *adapting quickly* refers to a few parameter updates. Here, we briefly describe the meta-learning approaches used in this work:

MAML [10]: Given an episode with K classes and an embedding function $f(\cdot, \theta)$, a learnable linear layer $clf(\cdot, \phi)$ is added on it and trained on the support set of the episode via gradient descent iterations, and evaluated on the query set. This step is performed independently for each episode, and the loss on the query set across all training episodes is aggregated. Which is then backpropagated through within-episode iterations to compute gradients of the query loss with respect to θ and ϕ . These gradient is then used to update the parameters, and this is referred to as the meta-update. However, this involves computing second-order derivatives, which can be computationally expensive. Hence, we use its first-order approximation, also known as fo-MAML [10], where the within-episode gradients are ignored during the meta-update.

Proto-MAML [31]: Proto-MAML is inspired by Prototypical networks [25], where a prototype \mathbf{p}_i for class c_i is the average of the embeddings of the samples of the class c_i in the support set. A query sample is classified as class c_i if the embedding of the sample is nearest to its prototype \mathbf{p}_i in the Euclidean space. Snell et al. [25] explains that prototypical networks can be re-interpreted as a linear layer applied on the embeddings from $f(\cdot, \theta)$ where the weights for the unit representing the class c_i is $\mathbf{w}_i = 2\mathbf{p}_i$ and bias is $b_i = -\|\mathbf{p}_i\|^2$. Proto-MAML uses this assignment of \mathbf{w}_i and b_i to initialize the parameters of $clf(\cdot, \phi)$. Here, we use the fo-MAML with the prototypical assignment of parameters of $clf(\cdot, \phi)$ and refer to this version as proto-fo-MAML.

3 Related Work

Detecting observed or imagined text from EEG has been actively studied in the literature. Some earlier works have achieved good performance in EEG-to-Text decoding with closed-vocabulary datasets containing very few classes [20, 22]. Recent works focus on open vocabulary EEG-to-Text decoding with thousands of classes, where they either attempt to reconstruct [18, 28, 34] or semantically summarize [19] the text a person views on a screen from the EEG signals. However, an EEG might not capture representations of each word, including all parts of speech, but it might capture representations of nouns corresponding to real objects. It is known that the human brain processes visual objects hierarchically [3, 5]. Here, we explore whether representations of objects in the brain induced via textual stimuli of the object follow a similar hierarchy.

As far as hierarchical modelling is concerned, the works of Zhu et al. [38] and Triantafillou et al. [31] are closely related to our work. Zhu et al. [38] created EEG-ImageNet, which is a dataset of EEG and image pairs across 80 classes, where 40 classes are coarse-grained, distinct classes from ImageNet [7], whereas the other 40 classes

come from 5 groups corresponding to concepts in WordNet with 8 categories each. However, EEG-ImageNet exhibits a very limited hierarchy comprising only 5 concepts from WordNet. In contrast, our test split contains 75 concepts, enabling a rigorous hierarchical study. Triantafillou et al. [31] performs a similar strategy as ours to build a hierarchy. However, our goal differs fundamentally in terms of using hierarchy-aware episodes as a probing tool to analyze neural representations under varying ontological abstraction, rather than training general-purpose few-shot learners. We also perform rigorous hierarchical studies given a rich hierarchy in the test split, unlike [31].

Regarding episodic Learning in the EEG decoding literature, most studies focus on cross-subject few-shot learning. As the EEG signal across subjects varies widely, they address this issue by treating each subject as an episode and applying episodic meta-learning, enabling the models to adapt quickly to novel subjects [1, 4, 9, 11]. In most cases, episodes have a limited labels that remain fixed across episodes. In a realistic scenario, this might not be the case; hence, we need a more realistic organization of episodes, for which we adopt a hierarchical structure.

4 Hierarchic-EEG2Text

In this section, we elaborate on how we build the framework for assessing EEG-to-Text decoding across hierarchical abstraction levels. We first briefly describe the dataset and the preprocessing pipeline, then describe building the concept hierarchy, and finally describe the episode sampling strategy.

4.1 Dataset

We used the PEERS dataset [14] for our experiments. The PEERS dataset consists of EEG signals recorded while subjects observed English words displayed on the screen (and later recalled them) under varying conditions in which they performed decision-making and arithmetic tasks, thereby inducing signal variability. The dataset consists of five major experiments grouped into 3 sections: *ltpFR*, *ltpFR2*, and *VFFR*, in which 300+ subjects contributed 7000+ sessions of 90 minutes each, observing words from a pool of 1638 English words. In this work, we have used *ltpFR* and *ltpFR2* groups, whose descriptions are provided in appendix Section A.

4.1.1 Alignment of Multiple Montage. EEG signals in the PEERS dataset were recorded using 3 different electrode layouts: (i) 129-channel GSN 200, (ii) 129-channel HydroCel GSN, and (iii) 128-channel BioSemi headcap. In this work, our main objective is to perform a hierarchical study of EEG-to-Text, rather than montage-agnostic EEG processing. Although we use a recent montage agnostic architecture, for a fair comparison with traditional EEG architectures, we select 96 channels so that all EEG data can be used in the study. For channel selection, we use one of the layouts as the reference layout and apply k -nearest neighbor to find the corresponding channel in the other layout. We do so because not all subjects have EEG electrode placement in exactly the same way. There will always be some variability in electrode placement across subjects and sessions due to differences in head shape and manual headset use. An electrode x may sometimes be placed closer to its neighbor y and sometimes farther apart. The detailed steps involved in the selection of the channels are outlined as follows:

Step 1: We consider the BioSemi ABC layout (used by the 128-channel BioSemi headcap) as the reference layout. For each electrode in the reference, we find 8-nearest neighbors in the other two (target) layouts using the known xyz -location of electrodes. This way we get a tuples in the form of (e_i^r, e_i^t) where e_i^r is an electrode in the reference layout and e_i^t is a list of neighbors in the target layout such that $e_{i,j}^t$ is the j^{th} nearest neighbor of e_i^r .

Step 2: There might be a case where two electrodes in the reference layout have the same nearest neighbor. In other words, for $i \neq j$, there may exist two tuples (e_i^r, e_i^t) and (e_j^r, e_j^t) such that $e_{i,1}^t = e_{j,1}^t$. We use the Euclidean distance $d(.,.)$ to resolve such conflicts, and repeat this step 8 times. If the nearest-neighbor list is exhausted to only 1 electrode, we skip that tuple during conflict resolution. If there are still duplicates, only one is retained.

Step 3: After de-duplication at step 2, we select all tuples such that there exists a nearest neighbor for a reference electrode in both the layouts.

4.1.2 Pre-processing. As we also study architectures pre-trained on the TUEG corpus [21, 33], we follow pre-processing steps similar to those used in [33], *i.e.*, (i) re-reference the data to the average, (ii) extract electrodes as per selection in Section 4.1.1 based on the layout, (iii) downsample to 200Hz, (iv) apply a band-pass filter from 0.3 – 75Hz, (v) set the unit to $100\mu V$. We used 1-sec EEG signal window for each word in the dataset.

4.2 Hierarchy of Concepts

In order to create a hierarchy of concepts, we used NLTK’s WordNet [2, 32] interface to build a Directed Acyclic Graph (DAG) using the *IS-A* relationship. Key steps involved in the creation of DAG are as follows:

Initializing the DAG. We consider all the words in the PEERS Dataset [14] as the leaves of the DAG. For each leaf node, we use the closest synonym from the synset returned by WordNet as the parent of the leaf node. Then, we use the hypernym-path from the root in WordNet to the given synonym to create the path from the root to the leaf. We discard all words whose synsets are not available in WordNet, resulting in a DAG with a single root, where each leaf node corresponds to a word in the dataset and each internal node represents a WordNet concept.

Removal of Broad Words. The set of words in the PEERS dataset contains several words that are too broad (*e.g. animal, mammal, creature, and so on*) and are placed close to the root. In our experiments, we considered words with narrower meanings and discarded broader ones similar to WordNet concepts. To identify such words, we compute the total number of siblings of each leaf node and subtract this number from the total number of leaf nodes reachable by the parent of the corresponding leaf node. If the result is too high (≥ 45), the word is possibly too broad. We remove such words from the DAG (check appendix Section B for related details).

DAGs for Train-Val-Test Split. For *meta-train* we use data from “ltp_FR” and for *meta-validation* and *meta-test*, we use the 576 words from the “ltp_FR2” group of the PEERS dataset. This choice ensures that each task has sufficient samples in both the support and query sets during episodic evaluation, as words in the “ltp_FR2” group are shown to each subject more times than those in the “ltp_FR”

group. We retain all (*word, subject*) pairs with ≥ 23 occurrences and remove these pairs from the *meta-train* split. The selected words and subjects are then randomly divided between the *meta-validation* and *meta-test* splits. Although initializing the DAG with all words helped filter out overly broad concepts, we reconstruct the DAG separately for each of the *meta-train*, *meta-validation*, and *meta-test* based only on the words assigned to that split. This results in a *meta-train* split with 1126 words, 204 subjects, and 484832 samples; a *meta-validation* split with 92 words, 15 subjects, and 32393 samples; and a *meta-test* split with 392 words, 45 subjects, and 414313 samples.

4.3 Episode Sampling

We use the episode sampling method similar to that in [31]. We present the key steps as follows:

Sampling Classes. For each DAG, we first identify the set of eligible internal nodes. We discard nodes that are too close to the root (see appendix Section B) and retain internal nodes having at least 5 reachable leaf nodes. We then uniformly sample one internal node from this eligible set and treat the leaf nodes reachable from it as the candidate classes. If the number of reachable leaf nodes is ≥ 10 , we randomly select 10 words as the classes; otherwise, we use the entire set of reachable leaves. We refer to the set of reachable leaves from an internal node as the "span" of the node, and to the span's size as the "span length".

Shots for Query Set. Number of samples per class for the query set is kept constant across all episodes and is determined by Equation (1).

$$k_q = \min\left\{10, \left(\min_{c \in C} [0.5 * |S(c)|]\right)\right\} \quad (1)$$

where $S(c)$ is the set of samples available for class c and C is set of classes sampled for the episode. Equation (1) ensures that at least half the samples for all classes considered in the episode are available for the support set.

Total Support Size. To avoid a too large support set, the number of samples for each class is limited to at most 100. Specifically, the total support size is determined by Equation (2).

$$|\mathcal{D}_{sup}| = \min\left\{100, \sum_{c \in C} [\beta * \min\{100, |S(c)| - k_q\}]\right\} \quad (2)$$

where β is uniformly sampled from $(0, 1]$, which ensures episodes of both large and small support sets.

Shots for Support Set. First, the proportion of available samples per class that would contribute to the support set is determined by the following normalized exponential function:

$$R_c = \frac{\exp(\alpha_c + \log(|S(c)|))}{\sum_{c' \in C} \exp(\alpha_{c'} + \log(|S(c')|))} \quad (3)$$

where α_c is uniformly sampled from $[\log(0.5), \log(0.2))$ which brings in some noise in the distribution. Finally, the shots per class are determined as:

$$k_{sup^c} = \min\{[R_c * (|\mathcal{D}_{sup}| - |C|)] + 1, |S(c)| - k_q\} \quad (4)$$

While sampling episodes for episodic training, we ensure that the support and query sets are disjoint not only within each episode but also across all episodes.

During episodic evaluation, we iterated through all the eligible internal nodes, and for each such node, we sampled I instances of episodes to ensure most leaves from the span are considered, where $I_{meta-validation} = 5$ and $I_{meta-test} = 10$. We report the mean and standard deviation of performances across all internal nodes.

4.4 Metrics

For all experiments, we have reported the "chance-adjusted accuracy" or the "normalized accuracy" for classification tasks, so that the evaluation scale remains the same across N -way classification tasks with varying N . The normalized accuracy for an N -way classification task is defined as:

$$Normalized\ Accuracy = \frac{A - \frac{1}{N}}{1 - \frac{1}{N}} * 100$$

Where A is either accuracy or balanced accuracy. A normalized accuracy of 0 is as poor as a random guess, while a negative value indicates performance poorer than a random guess. The closer the value is to 100, the better.

5 Experiments and Results

Our primary objective is to study EEG-to-Text decoding at various hierarchical levels. Through our experiments, we show that performing non-episodic evaluation with a large number of classes can be difficult for DNN models and that hierarchical episodic evaluation yields insights into various levels of abstraction. We perform our experiments on three architectures: (i) EEGNet [17] is a traditional EEG decoding architecture mainly built of convolution layers, (ii) NICE-EEG [26] is a modern EEG decoding architecture built with a spatial transformer followed by convolution layers, and (iii) CBraMod [33] is a foundational model pretrained on a large EEG corpus. We used CBraMod, both with pre-trained (w PT) and without pre-trained (w/o PT) weights, to study the effect of self-supervised pretraining.

5.1 Episodic Evaluation

For episodic evaluation, we trained the architectures in two different setups covering three algorithms: (i) Baseline, where we train the architectures with all the classes of *meta-train* together as a typical classification task in a non-episodic manner, but perform validation and evaluation in an episodic manner as described in Section 4.3, (ii) Episodic learning, where we train the architectures using fo-MAML and proto-fo-MAML.

Table 1 specifies overall episodic performance for 2-way, 6-way, and 10-way episodes. This also reflects the episodic performance on unseen classes and subjects, as the sets of classes and subjects for *meta-train*, *meta-val*, and *meta-test* are disjoint. The key observations are that object categorization from brain-wide EEG activity during real-world tasks is very challenging, and that there is modest improvement in performance compared to non-episodic evaluation, as shown in Table 3, suggesting better performance in some episodes. The near-chance performance, specifically on 6-way and 10-way classification tasks, could be due to the greater complexity and variability of EEG signals when subjects engage in real-world reasoning. In some trials, the words were displayed without additional tasks, while in others, decision tasks involving animacy and

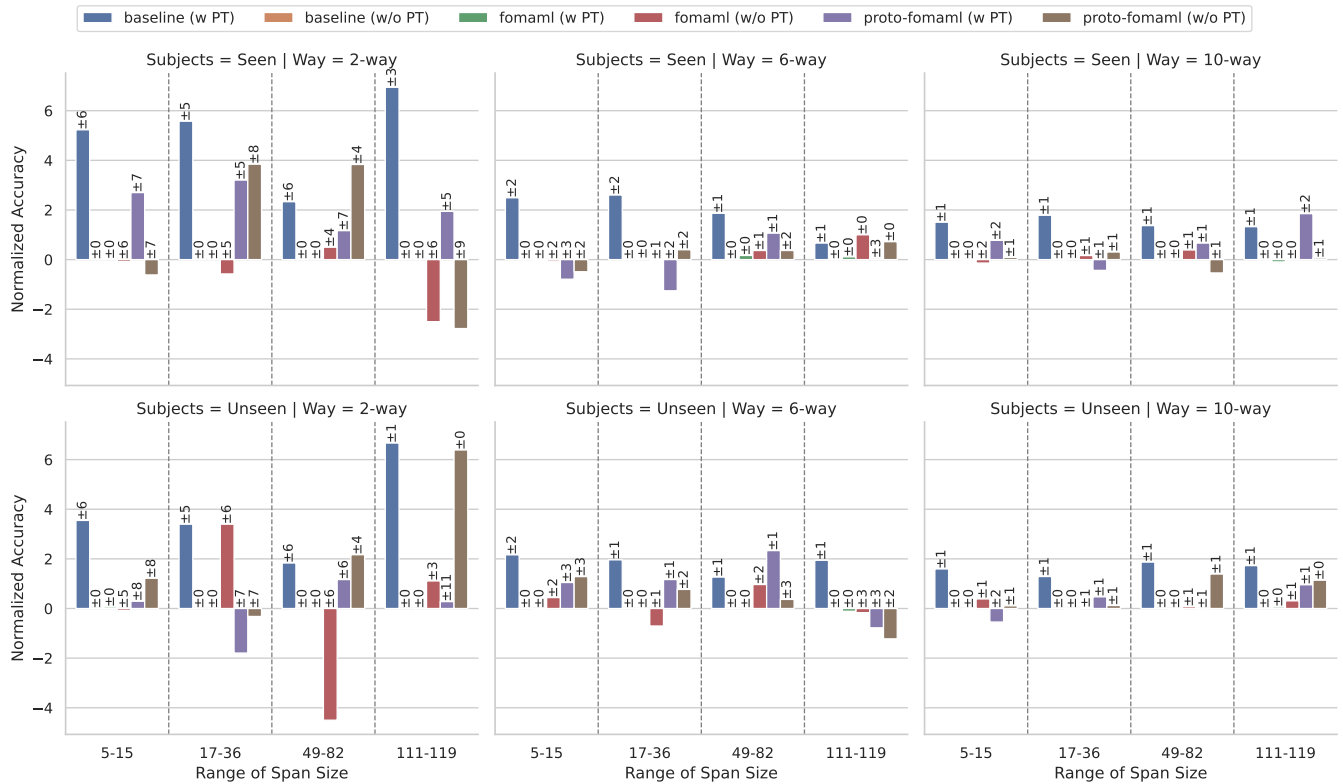


Figure 1: Span Analysis for episodic evaluation of CBraMod. It depicts the effects of an episode’s hierarchical depth on performance. Higher span size indicates coarse-grained episodes, and lower span size indicates fine-grained episodes.

size properties were included. This highlights the need for further advances in EEG decoding architectures to tackle such variability. Secondly, the baseline setup outperforms both meta-learning algorithms, despite their designs for multi-task learning that involve such variability. Another key observation is that CBraMod with pretrained weights performs best, while CBraMod trained from scratch without pretrained weights performs worst due to overfitting, indicating the benefit of large-scale self-supervised pre-training. The consistent advantage of pretrained baselines over meta-learning suggests that representation quality dominates adaptation in high-noise EEG settings. Meta-learning may amplify noise when task boundaries are weakly defined. Similar results have been found for episodic learning for images, where a self-supervised pretrained model performs better than sophisticated meta-learning algorithms [29].

Beyond these reasons, we want to emphasize again that the stimuli and tasks in the PEERS dataset reflect real-world reasoning and are also closer to clinical applications. Brain activity in PEERS is likely to be more abstract and complex than that of image/video EEG datasets (e.g. SEED [8, 37], SEED-IV [36], EEGCVPR40 [27], ThoughtViz [15, 16]), etc, where visual stimuli evoke wider and more stereotyped brain activity [35] and benefit ML models for categorization. We believe that our evaluation brings forth the challenges of meta-learning on EEG datasets with more complex tasks.

We also evaluated performance on 9 seen subjects from the *ltpFR* group of the PEERS dataset, which had classes included in the *meta-test*. Although these subjects were observed by the model during training, the set of classes still remained disjoint. Table 2 specifies the episodic performance for the seen subjects. While most observations remain the same as for unseen subjects, overall performance increased specifically for CBraMod with pretrained weights.

Another key observation here is that the standard deviation is quite high in the performance aggregated across all the internal nodes, which indicates that the model may have performed better for some episodes/concepts, while for some, it performed poorer, which highlights the need for more fine-grained analysis, which we discuss in the next section.

5.2 Hierarchical Analysis

The results in the previous section provide a coarse-grained view of the EEG-to-Text decoding across episodes. Here, we attempt to provide a fine-grained view via: (i) Span Analysis, where we study performance at different depths of concepts, and (ii) Abstraction Analysis, where we pick classes from different levels of the hierarchy DAG. For the upcoming sections, we use CBraMod due to its superior performance.

5.2.1 Span Analysis. As defined earlier, we refer to the set of reachable leaves from an internal node as the "span" of that node in the

Table 3: Normalized (balanced) accuracy on joint evaluation with 1126 classes, together with a stratified train-val-test split.

EMBEDDER	TRAIN	TEST
EEGNET [17]	0.03	0.00
NICE EEG [26]	53.24	0.01
CBRAMOD [33] (w/o PT)	0.00	0.00
CBRAMOD [33] (w PT)	1.55	0.02

cloud visualization gives a clear view of the observation in Figure 1 for the unseen subjects. Broader concepts (like `artifact.119`, `organism.111`, `living_thing.111`) perform well in 2-way classification, but their performance dips for 6-way and 10-way as the brightness of the concepts in the word cloud dips. Another key observation from Figure 1 is that the performance for CBraMod (w PT) for baseline learning is the lowest for the moderately broader concepts in 2-way task, suggesting the presence of very similar classes in the span set. As per Figure 2, this group includes concepts like `causal_agent.72`, `person.62`, `matter.49` that have very similar classes. For example, the intersection of the span set of `causal_agent.72` and `person.62` contains classes like ACTOR, ACTRESS, HOSTESS, GIRL, DAUGHTER, DANCER, etc, which just depict an image of a person. Similarly, most words in the span set of `matter.49` represents some kind of food items (check appendix Section D for full list), and differentiating such items via EEG representations can be a difficult task, which explains the low performance.

5.2.2 Abstraction Analysis. In this section, we study how classes at different levels of the hierarchy contribute to EEG-to-Text decoding. In all the previous sections, we used the leaf node of the DAG as the classes in the classification task. Here, we select the concepts represented by internal nodes that are ancestors of the leaf nodes with h hops in between them. If $h = 1$, then we prune all the leaf nodes and consider the new leaves as the classes, and we refer to the new set of classes as $L - 1$. If $h = 2$, we prune twice and refer to the resulting set of classes as $L - 2$. After pruning, we assign samples to the new classes using the ancestor-descendant mapping between the old and new leaves. Towards this end, we considered three sets of classes: $L - 2$, $L - 3$, and $L - 4$. For each set, we trained the model independently using all learning methods and evaluated performance episodically. An important point to note is that when classes are selected from the leaves without any pruning, the classes are disjoint across *meta-train*, *meta-validation*, and *meta-test*. However, when we prune the DAG, the set of classes begins to overlap across the splits. Specifically, $\sim 25\%$ of test classes overlapped with that of the train classes for all three sets $L - 2$, $L - 3$, and $L - 4$. Figure 3 visualizes the episodic performance of CBraMod on the three sets trained with various learning approaches. As in earlier results, the baseline learning method performs consistently, while meta-learning remains unstable and shows no trend. However, for the baseline method, overall performance increases in most cases. Specifically, when CBraMod is trained without pretraining, its performance improves at $L - 4$. Moreover, it beats the case when CBraMod is initialized with pretrained weights. This observation

yields two insights: (i) the possibility of more distinct classes as we move a few hops above the last level of the hierarchy, and (ii) improvement in the results at $L - 4$ indicates that EEG representations are sensitive to levels of abstraction in the ontological hierarchy.

We emphasize that absolute performance remains near chance, and variance is high across episodes. Our goal is not to demonstrate strong decoding accuracy, but to analyze relative trends across controlled hierarchical conditions under identical evaluation protocols.

5.3 Non-Episodic Evaluation

In this experiment, we train and evaluate the architectures in a non-episodic manner, where we use the data under *meta-train* and divide them into stratified *train-validation-test* splits (note that *meta-train*, *meta-val*, and *meta-test* splits are meant for episodic learning only). We train the architectures to map EEG samples to 1126 classes, and the set of classes remains the same for both training and evaluation, as described in Section 2.1.1. The Table 3 specifies the performance of the architectures in the train and test sets in terms of normalized balanced accuracy (mean of recall for all classes).

We observe that all architectures fail to generalize to the test set. This highlights the difficulty of classifying signals into a large set of classes. One possible reason is that certain words (or leaf nodes) under the same internal node in the DAG may share high semantic similarity (see Figure 4 in the appendix for an example). EEG might not capture representations for each of them, and multiple such instances make the classification task difficult when all classes are considered together. On the other hand, as we show in Section 5.1, performing an independent classification task for such nodes by treating their span sets as classes may yield different results, as the span sets of some nodes may contain more distinct objects compared to others.

6 Limitations and Ethical Considerations

In this work, we focus on hierarchical analysis of EEG-to-Text decoding to understand how EEG captures object representations in the brain that correspond to textual stimuli. We used the PEERS [14] dataset, which contains large classes of real objects. However, even the most modern architecture, such as CBraMod, performed close to chance level, according to our findings.

This may have occurred because of high variability in the dataset, as the subjects also performed additional tasks while viewing words corresponding to objects. This implies that the current methods fail to capture representations from EEG alone and may require support from other modalities. In this direction, it would be interesting to study how aligning EEG representations with other modalities, such as textual representations, would help. As a part of future work, we plan to explore this direction to provide more robust insights. Additionally, we will explore other vision-based datasets on which ML models have achieved higher accuracy, to evaluate the benefits of meta-learning and ontological priors.

Regarding ethical considerations, we haven't recorded physiological signals; instead, we used a publicly available dataset. Information about subjects is already anonymized by the dataset authors, and we ensure that our methodology doesn't extract any information that can be used to identify subjects.

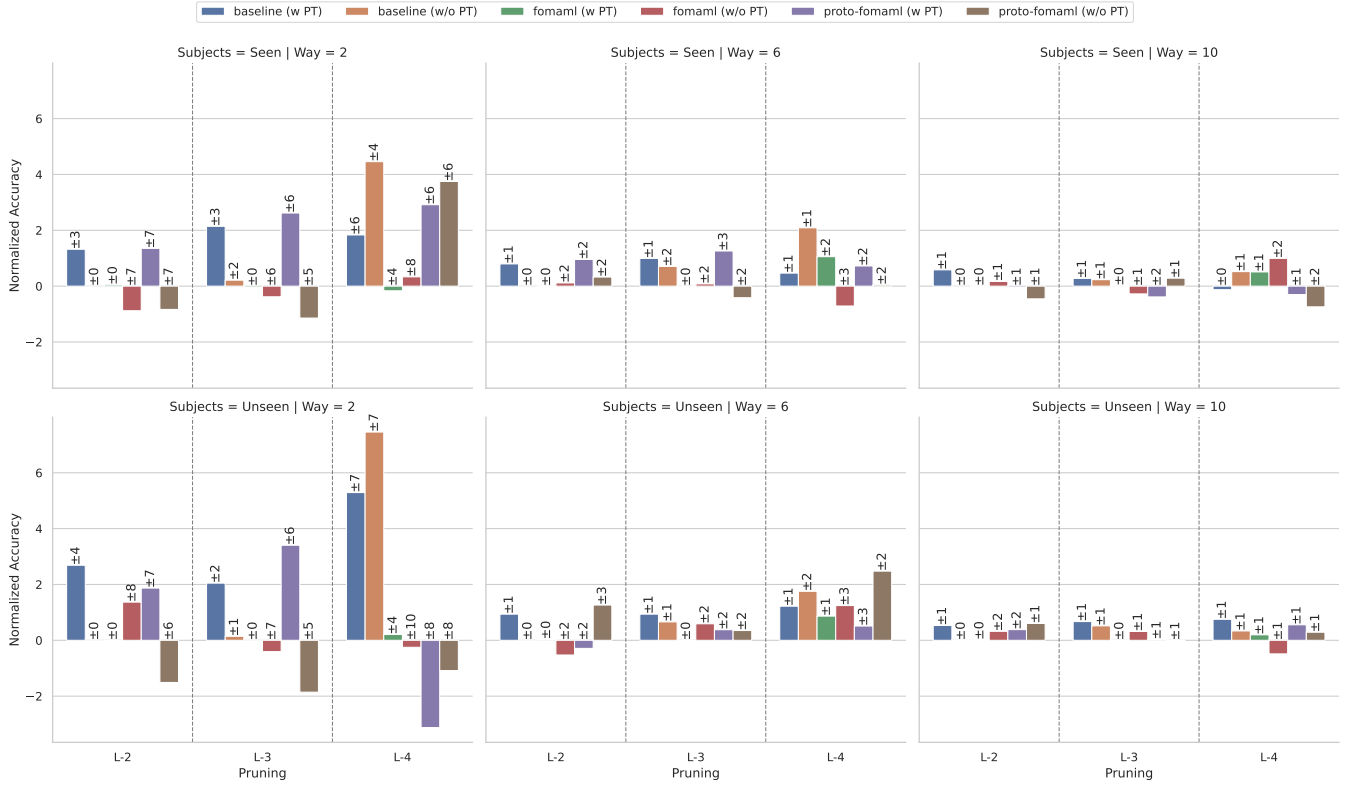


Figure 3: Abstraction Analysis for episodic evaluation of CBraMod. Value of h in $L - h$ specifies the number of pruning steps performed on the DAG. As the value of h increases, more abstract classes are considered.

7 Conclusion

In this work, we study EEG-to-Text decoding across hierarchical abstraction levels. We show that classifying EEG signals into a large set of classes corresponding to their respective textual stimuli can be difficult, as some objects may share very similar meanings. EEG, as a standalone signal, might not capture subtle details across similar objects, but it may have a more abstract representation of them. Hence, we propose to study EEG-to-Text decoding in an episodic manner, with episodes sampled hierarchically. Firstly, we found that while non-episodic evaluation fails, the model performs better when evaluated episodically, indicating the presence of hierarchical representations in EEG. Secondly, we observed that coarse-grained tasks were easier than fine-grained tasks, but this was true only for binary classification. As we bring more classes to the task, both fine-grained and coarse-grained tasks become equally difficult. Another key finding is that models perform better when we attempt mapping signals to abstract classes (e.g., instead of considering BOY, GIRL, MAN, WOMAN as different classes, consider them as one class - PERSON). This suggests that EEG representations are sensitive to abstraction.

Additionally, by adopting an episodic approach, we created the largest episodic evaluation framework in the EEG domain, facilitating the ML community in developing efficient episodic learning algorithms for EEG decoding tasks. In this regard, we found that self-supervised pretrained models can outperform complex meta-learning techniques in EEG-to-Text decoding.

Our research highlights the importance of abstraction depth in the context of EEG-to-Text decoding. We hope this work will inspire further studies to enhance the efficacy of EEG-based applications across various fields.

Acknowledgments

We would like to thank Atharv Nangare from IIT Gandhinagar for introducing us to the PEERS dataset and for the time he spent discussing its applications.

References

- [1] Swapnil Bhosale, Rupayan Chakraborty, and Sunil Kumar Koppurapu. 2022. Calibration free meta learning based approach for subject independent EEG emotion recognition. *Biomedical Signal Processing and Control* 72 (2022), 103289.
- [2] Steven Bird. 2006. NLTK: the natural language toolkit. In *Proceedings of the COLING/ACL 2006 interactive presentation sessions*. 69–72.
- [3] Thomas Carlson, David A Tovar, Arjen Alink, and Nikolaus Kriegeskorte. 2013. Representational dynamics of object vision: the first 1000 ms. *Journal of vision* 13, 10 (2013), 1–1.
- [4] Cheng Chen, Hao Fang, Yuxiao Yang, and Yi Zhou. 2025. Model-agnostic meta-learning for EEG-based inter-subject emotion recognition. *Journal of Neural Engineering* 22, 1 (2025), 016008.
- [5] Radoslaw Martin Cichy, Dimitrios Pantazis, and Aude Oliva. 2014. Resolving human object recognition in space and time. *Nature neuroscience* 17, 3 (2014), 455–462.
- [6] Mike X Cohen. 2014. *Analyzing neural time series data: theory and practice*. MIT press.
- [7] Jia Deng, Wei Dong, Richard Socher, Li-Jia Li, Kai Li, and Li Fei-Fei. 2009. Imagenet: A large-scale hierarchical image database. In *2009 IEEE conference on computer vision and pattern recognition*. Ieee, 248–255.

- [8] Ruo-Nan Duan, Jia-Yi Zhu, and Bao-Liang Lu. 2013. Differential entropy feature for EEG-based emotion classification. In *6th International IEEE/EMBS Conference on Neural Engineering (NER)*. IEEE, 81–84.
- [9] Tieshang Duan, Mohammad Abuzar Shaikh, Mihir Chauhan, Jun Chu, Rohini K Srihari, Archita Pathak, and Sargur N Srihari. 2020. Meta learn on constrained transfer learning for low resource cross subject EEG classification. *IEEE Access* 8 (2020), 224791–224802.
- [10] Chelsea Finn, Pieter Abbeel, and Sergey Levine. 2017. Model-agnostic meta-learning for fast adaptation of deep networks. In *International conference on machine learning*. PMLR, 1126–1135.
- [11] Ji-Wung Han, Soyeon Bak, Jun-Mo Kim, Woohyeok Choi, Dong-Hee Shin, Young-Han Son, and Tae-Eui Kam. 2024. Meta-eeg: Meta-learning-based class-relevant eeg representation learning for zero-calibration brain-computer interfaces. *Expert Systems with Applications* 238 (2024), 121986.
- [12] Nora Hollenstein, Jonathan Rotsztein, Marius Troendle, Andreas Pedroni, Ce Zhang, and Nicolas Langer. 2018. ZuCo, a simultaneous EEG and eye-tracking resource for natural sentence reading. *Scientific data* 5, 1 (2018), 1–13.
- [13] Nora Hollenstein, Marius Troendle, Ce Zhang, and Nicolas Langer. 2020. ZuCo 2.0: A dataset of physiological recordings during natural reading and annotation. In *Proceedings of the Twelfth Language Resources and Evaluation Conference*. 138–146.
- [14] Michael J. Kahana, Joseph H. Rudoler, Lynn J. Lohnas, Karl Healey, Ada Aka, Adam Broitman, Elizabeth Crutchley, Patrick Crutchley, Kylie H. Alm, Brandon S. Katerman, Nicole E. Miller, Joel R. Kuhn, Yuxuan Li, Nicole M. Long, Jonathan Miller, Madison D. Paron, Jesse K. Pazdera, Isaac Pedisich, and Christoph T. Weidemann. 2023. "Penn Electrophysiology of Encoding and Retrieval Study (PEERS)". doi:doi:10.18112/openneuro.ds004395.v2.0.0
- [15] Blair Kaneshiro, Marcos Perreau Guimaraes, Hyung-Suk Kim, Anthony M Norcia, and Patrick Suppes. 2015. A representational similarity analysis of the dynamics of object processing using single-trial EEG classification. *Plos one* 10, 8 (2015), e0135697.
- [16] Pradeep Kumar, Rajkumar Saini, Partha Pratim Roy, Pawan Kumar Sahu, and Debi Prosad Dogra. 2018. Envisioned speech recognition using EEG sensors. *Personal and Ubiquitous Computing* 22, 1 (2018), 185–199.
- [17] Vernon J Lawhern, Amelia J Solon, Nicholas R Waytowich, Stephen M Gordon, Chou P Hung, and Brent J Lance. 2018. EEGNet: a compact convolutional neural network for EEG-based brain-computer interfaces. *Journal of neural engineering* 15, 5 (2018), 056013.
- [18] Hanwen Liu, Daniel Hajjaligol, Benny Antony, Aiguo Han, and Xuan Wang. 2024. Eeg2text: Open vocabulary eeg-to-text decoding with eeg pre-training and multi-view transformer. *arXiv preprint arXiv:2405.02165* (2024).
- [19] Xiaozhao Liu, Dinggang Shen, and Xihui Liu. 2025. Learning Interpretable Representations Leads to Semantically Faithful EEG-to-Text Generation. *arXiv preprint arXiv:2505.17099* (2025).
- [20] Nicolás Nieto, Victoria Peterson, Hugo Leonardo Rufiner, Juan Esteban Kamienkowski, and Ruben Spies. 2022. Thinking out loud, an open-access EEG-based BCI dataset for inner speech recognition. *Scientific data* 9, 1 (2022), 52.
- [21] Iyad Obeid and Joseph Picone. 2016. The temple university hospital EEG data corpus. *Frontiers in neuroscience* 10 (2016), 196.
- [22] Pramit Saha, Muhammad Abdul-Mageed, and Sidney Fels. 2019. Speak Your Mind. *Towards Imagined Speech Recognition With Hierarchical Deep Learning* (2019).
- [23] Prajwal Singh, Dwip Dalal, Gautam Vashishtha, Krishna Miyapuram, and Shanmuganathan Raman. 2024. Learning robust deep visual representations from eeg brain recordings. In *Proceedings of the IEEE/CVF Winter Conference on Applications of Computer Vision*. 7553–7562.
- [24] Prajwal Singh, Pankaj Pandey, Krishna Miyapuram, and Shanmuganathan Raman. 2023. EEG2IMAGE: image reconstruction from EEG brain signals. In *ICASSP 2023-2023 IEEE International Conference on Acoustics, Speech and Signal Processing (ICASSP)*. IEEE, 1–5.
- [25] Jake Snell, Kevin Swersky, and Richard Zemel. 2017. Prototypical networks for few-shot learning. *Advances in neural information processing systems* 30 (2017).
- [26] Yonghao Song, Bingchuan Liu, Xiang Li, Nanlin Shi, Yijun Wang, and Xiaorong Gao. 2023. Decoding natural images from eeg for object recognition. *arXiv preprint arXiv:2308.13234* (2023).
- [27] Concetto Spampinato, Simone Palazzo, Isaak Kavasidis, Daniela Giordano, Nasim Souly, and Mubarak Shah. 2017. Deep learning human mind for automated visual classification. In *Proceedings of the IEEE conference on computer vision and pattern recognition*. 6809–6817.
- [28] Yitian Tao, Yan Liang, Luoyu Wang, Yongqing Li, Qing Yang, and Han Zhang. 2025. See: Semantically aligned eeg-to-text translation. In *ICASSP 2025-2025 IEEE International Conference on Acoustics, Speech and Signal Processing (ICASSP)*. IEEE, 1–5.
- [29] Yonglong Tian, Yue Wang, Dilip Krishnan, Joshua B Tenenbaum, and Phillip Isola. 2020. Rethinking few-shot image classification: a good embedding is all you need?. In *European conference on computer vision*. Springer, 266–282.
- [30] Praveen Tirupattur, Yogesh Singh Rawat, Concetto Spampinato, and Mubarak Shah. 2018. Thoughtviz: Visualizing human thoughts using generative adversarial network. In *Proceedings of the 26th ACM international conference on Multimedia*. 950–958.
- [31] Eleni Triantafyllou, Tyler Zhu, Vincent Dumoulin, Pascal Lamblin, Utku Evci, Kelvin Xu, Ross Goroshin, Carles Gelada, Kevin Swersky, Pierre-Antoine Manzagol, et al. 2019. Meta-dataset: A dataset of datasets for learning to learn from few examples. *arXiv preprint arXiv:1903.03096* (2019).
- [32] Princeton University. 2019. WordNet | A Lexical Database for English. <https://wordnet.princeton.edu/>
- [33] Jiquan Wang, Sha Zhao, Zhiling Luo, Yangxuan Zhou, Haiteng Jiang, Shijian Li, Tao Li, and Gang Pan. 2024. Cbrmod: A criss-cross brain foundation model for eeg decoding. *arXiv preprint arXiv:2412.07236* (2024).
- [34] Zhenhailong Wang and Heng Ji. 2022. Open vocabulary electroencephalography-to-text decoding and zero-shot sentiment classification. In *Proceedings of the AAAI Conference on Artificial Intelligence*, Vol. 36. 5350–5358.
- [35] Daniel LK Yamins, Ha Hong, Charles F Cadieu, Ethan A Solomon, Darren Seibert, and James J DiCarlo. 2014. Performance-optimized hierarchical models predict neural responses in higher visual cortex. *Proceedings of the national academy of sciences* 111, 23 (2014), 8619–8624.
- [36] W. Zheng, W. Liu, Y. Lu, B. Lu, and A. Cichocki. 2018. EmotionMeter: A Multimodal Framework for Recognizing Human Emotions. *IEEE Transactions on Cybernetics* (2018), 1–13. doi:10.1109/TCYB.2018.2797176
- [37] Wei-Long Zheng and Bao-Liang Lu. 2015. Investigating Critical Frequency Bands and Channels for EEG-based Emotion Recognition with Deep Neural Networks. *IEEE Transactions on Autonomous Mental Development* 7, 3 (2015), 162–175. doi:10.1109/TAMD.2015.2431497
- [38] Shuqi Zhu, Ziyi Ye, Qingyao Ai, and Yiqun Liu. 2024. Eeg-imagenet: An electroencephalogram dataset and benchmarks with image visual stimuli of multi-granularity labels. *arXiv preprint arXiv:2406.07151* (2024).

A Dataset

The PEERS dataset was recorded via 5 major recording experiments out of which we used the data of 4 experiments whose description is provided below:

Experiment 1 and 3: Each session in the experiment consists of a series of 16 trials, each involving 16 visually presented words, followed by a recall task in which subjects recall as many words as they can. Each word is presented for 3s, with an inter-stimulus interval (ISI) ranging from 0.8s to 1.2s. Each session consists of three kinds of trials - (i) 4 *No Task Trials*, where subject observes the presented words, (ii) 8 *Task Trials*, where in 4 of the trials a subject decide if the object represented by the presented word fit in a shoebox (also known as size task) and in the remaining 4 trials a subject decide if the object is living being (also known as animacy task), and (iii) 4 *Task-Shift Trials*, where both the size and animacy task exists within the same trial. Experiment 3 differs from experiment 1 in the recall task, where in experiment 3, a subject also verbalizes the words they recall.

Experiment 2: This experiment introduces distractor intervals in addition to the word-based intervals in a trial. In the distractor interval, a math problem appeared on the screen in the form of $A + B + C = ?$ where A , B , and C are positive single-digit numbers.

Experiment 4: Experiment 4 used a pool of 576 words selected from the original pool. Each word is displayed to all 98 subjects involved in this experiment. Each session had 24 trials, with each trial presenting 24 words individually for 1.6s, with ISI ranging from 0.8s to 1.2s, followed by a distractor interval.

Experiments 1, 2, and 3 of the PEERS dataset is also referred as (*ltpFR*) and experiment 4 as (*ltpFR2*).

B Discarded Labels and Nodes in DAG

The word "BLUEJAY" had no synonym in WordNet. Discarded words having too broad meaning are listed below, where the first

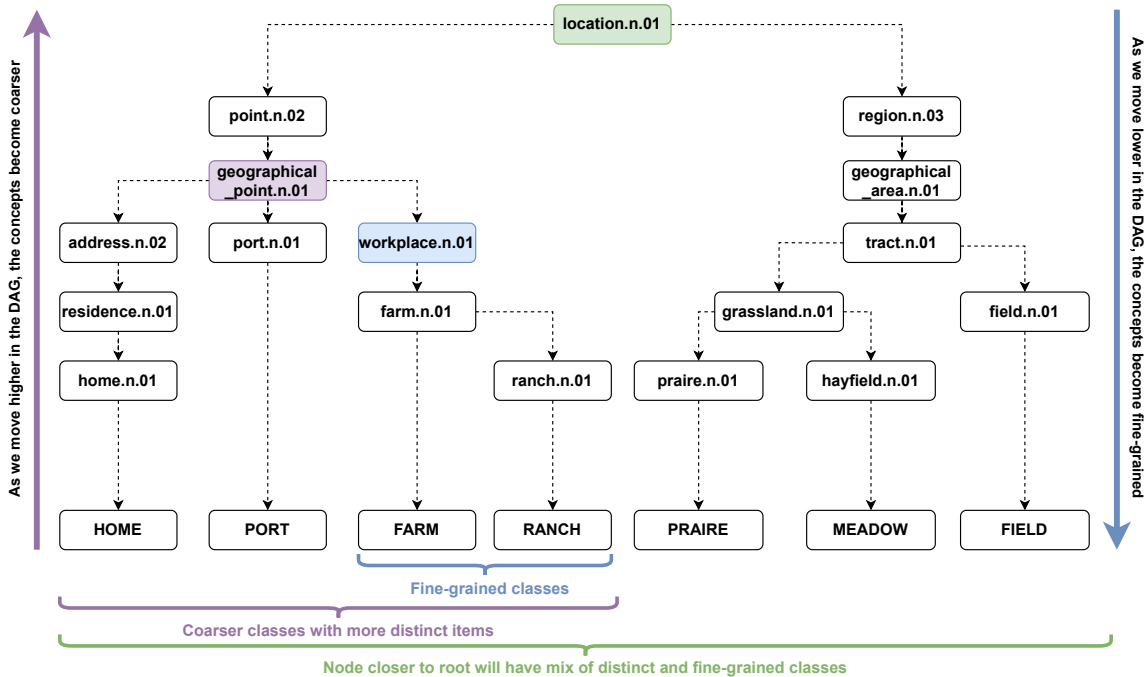


Figure 4: Subgraph of the DAG for meta-train split showing leaf nodes sharing the same internal node having high similarity in meaning (e.g., FARM, RANCH). In the presence of multiple such instances, EEG might not capture representations for each of them, making non-episodic EEG-to-Text classification with all labels together a difficult task.

value in the braces specifies the number of leaf nodes spanned by its parent, and the second value specifies the number of siblings:

- CREATURE (121, 9)
- ANIMAL (121, 9)
- PERSON (278, 58)
- BEAST (121, 9)
- MAMMAL (56, 2)

The discarded internal nodes correspond to the following synonyms/concepts: ‘whole.n.02’, ‘object.n.01’, ‘physical_entity.n.01’. The removal of these nodes also leads to the removal of 22 more words (still retaining ~ 98% of total words in the PEERS Dataset).

C Hyperparameter Settings

In this section, we provide details related to the experiment setup. Table 4 and table 5 provide the hyper-parameter settings used for training the models via non-episodic and episodic learning, respectively.

D Words Under Moderately Broad Concepts

This section lists the words under the span set of moderately broad concepts.

matter.49: SALAD, MAPLE, PUDDING, COFFEE, ORANGE, PASTA, BRANDY, GRAPE, PORK, PLASTER, PAPER, KLEENEX,

Table 4: Hyperparameter settings for experiments with non-episodic evaluation

Hyperparameters	Settings
Embedding dim	1024
Dropout	0.05
Learning rate	0.0003
Epoch	50
Weight Decay	0.001
Optimizer	AdamW

BEAVER, BARLEY, LAVA, TREAT, GARBAGE, PIZZA, SUPPER, CANDY, OZONE, JELLO, HONEY, MEAT, DRUG, LUNCH, POISON, PASTRY, SODA, TROUT, QUAIL, SNACK, OINTMENT, SLIME, CUSTARD, CIGAR, JELLY, POWDER, SPONGE, SALT, ATOM, GLASS, CHAMPAGNE, COCKTAIL, KETCHUP, APPLE, BACON, RADISH, GREASE

causal_agent.72: VIKING, REBEL, SPHINX, VIRUS, CONVICT, FRIEND, MUMMY, PRINCESS, DIVER, PATIENT, LODGE, BRANDY, INFANT, BABY, WIFE, WASHER, PISTON, HIKER, SERVER, DENTIST, HUSBAND, HOSTESS, CAPTIVE, SISTER, DANCER, WOMAN, JUGGLER, LOVER, DRIVER, DRUG, ACTOR, AGENT, SIBLING,

Table 5: Hyperparameter settings for experiments with episodic evaluation

Learning Method	Hyperparameters	Settings
Common to both	Embedding Dim	512
	Dropout	0.05
Baseline	Learning Rate	0.0003
	Epochs	50
	Batch Size	128
	Optimizer	AdamW
Meta-Learning	Outer Learning Rate	0.0003
	Inner Learning Rate	0.01
	No. of inner updates	5
	Inner Optimizer	Gradient Descent
	Outer Optimizer	Adam
	Total Meta Steps	5351
	Number of episodes in a Batch	4

CATCHER, DINER, GIRL, PUPIL, LADY, INMATE, SPOUSE, WAITRESS, DAUGHTER, GANGSTER, ACTRESS, MARINE, TEACHER,

OINTMENT, SERVANT, EXPERT, CASHIER, CIGAR, KEEPER, HOOD, CHEMIST, CHAUFFEUR, VAGRANT, POET, NOMAD, COCKTAIL, CHAMPAGNE, MAILMAN, PILOT, PRINCE, WORKER, PARTNER, WITNESS, BANKER, PREACHER, TYPIST, DONOR, OUTLAW, TOASTER

person.62: VIKING, REBEL, SPHINX, CONVICT, FRIEND, MUMMY, PRINCESS, DIVER, PATIENT, LODGE, INFANT, BABY, WIFE, WASHER, PISTON, HIKER, SERVER, DENTIST, HUSBAND, HOSTESS, CAPTIVE, SISTER, DANCER, WOMAN, JUGGLER, LOVER, ACTOR, SIBLING, CATCHER, DINER, GIRL, PUPIL, LADY, INMATE, SPOUSE, WAITRESS, DAUGHTER, GANGSTER, ACTRESS, MARINE, TEACHER, SERVANT, EXPERT, CASHIER, KEEPER, HOOD, CHEMIST, VAGRANT, POET, NOMAD, MAILMAN, PILOT, PRINCE, WORKER, PARTNER, WITNESS, BANKER, PREACHER, TYPIST, DONOR, OUTLAW, TOASTER